Effect of vanadium admixing on the surface structure of TiO2(110) under non-oxidizing conditions

Xin Song, Elena Primorac, Helmut Kuhlenbeck* and Hans-Joachim Freund

Fritz Haber Institute of the Max Planck Society, Chemical Physics Department, Faradayweg 4-6, 14195 Berlin, Germany

*Corresponding Author. E-mail: kuhlenbeck@fhi-berlin.mpg.de Tel: +49-30-8413-4222

ABSTRACT: Single crystalline Ti + V mixed oxide layers have been prepared by doping vanadium into TiO2(110) thin films on TiO2(110) single crystal substrates with a Ti + Ta mixed oxide interlayer between the film and the substrate. The interlayer prevents the diffusion of vanadium into the substrate and also the diffusion of Ti^{3+} between substrate and overlayer. Mixing vanadium into the TiO2 lattice increases the reducibility of the host oxide as concluded from an appreciable degree of reduction produced by comparatively mild annealing. A high density of bridging oxygen vacancies was identified at the surface of films with a low vanadium content (2%) while a (1 × 2) reconstruction as also known for massively reduced TiO2(110) was observed for layers with 8% of vanadium. Studies of methanol adsorption indicate that the vanadium atoms are mostly located below the surface since there is no indication of a vanadium-methanol interaction. We provide evidence that the reducibility of the vanadium ions in the thin film is higher than that of the titanium ions and we suggest that this is the origin of the increased reducibility of the mixed oxide.

Keywords: TiO2(110); vanadium admixing; surface structure; reactivity; reducibility; methanol.

1. Introduction

Dopants can have a substantial effect on the catalytic properties of an oxide as shown by theoretical and experimental studies [1–4]. Already half a century ago it was shown that Ni-

doped MgO powder samples are more active for N_2O decomposition than pure MgO [5]. Dopant atoms modify the properties of the atoms in the surrounding crystal volume. They may affect the crystal structure and may act as sources or sinks for electron charge which may strongly affect the catalytic properties [6–9]. Well-defined single crystalline models of real-life catalysts are well suited to study such effects at an atomic level due to the reduced complexity of such systems [4,10]. For instance, the activation of oxygen to a superoxo species by molybdenum atoms in CaO(001) was studied in detail with STM (scanning tunneling microscopy) and DFT (density functional theory) showing that a charge transfer involving the molybdenum atoms is responsible for this activation [8]. Dopants can also donate charge to deposited clusters, thereby changing their structure and probably also their catalytic properties as shown for the case of gold clusters on Mo doped CaO(100) [9]. The action of dopants is a rather general aspect of catalytic processes at surfaces and therefore an ongoing research activity in this field may be expected.

While TiO_2 single crystal surfaces are used mainly as supports in model catalyst studies [11–14], the modification of TiO_2 by dopants with the aim to enhance its catalytic/photocatalytic properties has also been investigated [15–17]. TiO_2 powder with cationic alkaline metal dopants (Li, Na, K and Cs) was found to catalyze acetone oligomerization [18], and anion dopants such as N and F were shown to affect the photo-catalytic efficiency of TiO_2 [15,19]. Nitrogen atoms doped into rutile and anatase single crystals with ion implantation methods were reported to promote the formation of oxygen vacancies [19], while Cr-doping of TiO_2(110) by calcination with Cr_2O_3 powder was found to increase the rate of surface oxygen vacancy formation [20]. In this work, we focus on the influence of a vanadium admixture on the properties of rutile TiO_2(110). A problem for the preparation of a vanadium admixture into TiO_2(110) is the high speed of vanadium diffusion in TiO_2 at elevated temperature (> 600 K), which leads to the loss of vanadium into the bulk of the TiO_2 single crystal if the vanadium admixture is prepared by vanadium deposition at the surface or admixture in near-surface regions [21,22]. In order to circumvent the vanadium diffusion problem, we have developed a recipe for the preparation of TiO_2(110) layers on TiO_2(110) single crystal substrates with a Ta + Ti mixed oxide diffusion barrier between the film and the substrate as described in a recent publication [23]. The diffusion barrier does not just block the diffusion of Ti^{3+} ions as discussed in reference [23], but also the diffusion of vanadium ions [24].

2. Experimental methods

2

The experiments were carried out with two different UHV systems. Both systems were equipped with ion guns for sample cleaning via Ar^+ ion sputtering, LEED (low energy electron diffraction) systems to check the surface order, electron beam evaporators (manufactured by Focus GmbH, Germany) for the deposition of vanadium, titanium and tantalum, and quartz microbalances for the calibration of the metal deposition rates.

High-resolution XPS spectra were recorded with a system located at the UE52-PGM-PES beamline of the BESSY II electron storage ring. The V 2p and Ti 2p XPS (X-ray photoelectron spectroscopy) data were recorded with a R4000 hemispherical electron energy analyzer (manufactured by VG-Scienta) employing photons with an energy of 630 eV. At a photon energy of 630 eV the surface sensitivity of V 2p and Ti 2p spectra is rather high [the electron IMFP (Inelastic mean free path) in TiO_2 is in the range of 5-6 Å according to the QUASES-IMFP program (downloadable from http://www.quases.com)]. Part of the spectra were recorded with an electron exit angle of 80° with respect to the surface normal which leads to an even higher surface sensitivity. The energy scale was calibrated by positioning the Au $4f_{7/2}$ level in a spectrum of a gold sheet at its literature value of 84 eV [25].

TPD (temperature programmed desorption) and STM (scanning tunneling microscopy) data were recorded in another UHV system which was additionally equipped with an EA125 electron energy analyzer (Omicron) for XPS. The room-temperature STM system was also manufactured by Omicron (model: STM1). STM images were measured with a bias voltage of 2.0 V and a tunneling current of 0.1 nA. The WSxM software was used to process the images [26]. The quadrupole mass spectrometer (Thermo Systems) used for TPD was mounted in a differentially pumped housing with a small (4 mm diameter) entrance opening (Feulner cup) [27]. During TPD measurements, the sample was positioned directly in front of this opening which significantly decreases the probability that gas molecules desorbing from the sample holder reach the mass spectrometer. TPD spectra with methanol as the probe molecule were recorded to test the reactivity of the mixed oxide. In these experiments 50 langmuirs (1 langmuir = 1×10^{-6} Torr·s) of methanol were dosed at room temperature and the spectra were recorded with a constant heating rate of 0.5 Ks^{-1}. Contributions of methanol to the spectra of masses 15 (methane), 18 (water) and 30 (formaldehyde) were subtracted prior to plotting according to $I_{plotted}^{compound} = I_{raw}^{compound} - C^{compound} I_{raw}^{methanol,mass\ 31}$, with the factor $C^{compound}$ being calculated from the mass fragmentation pattern of methanol and sensitivity factors published by the manufacturer of the mass spectrometer, and I denoting intensities.

The TiO$_2$(110) single crystal substrates were prepared by sputtering and annealing cycles consisting of sputtering with Ar$^+$ ions (1 keV, 5 μA) for 30 min at room temperature followed by annealing at 970 K in vacuum. These cycles were repeated until LEED images exhibited sharp spots with a low background intensity and XPS spectra did not show recognizable peaks other than those of TiO$_2$. After the initial preparation, the crystals had a light blue color which grew darker in the course of the experiments due to the annealing cycles required in further preparation steps. We note that this did not have a significant influence on the quality of the layers due to the presence of the Ti + Ta diffusion blocking barrier.

After substrate preparation, the Ti + Ta blocking layer (Ti$_{0.8}$Ta$_{0.2}$O$_2$, 30 Å thick) was prepared by co-deposition of Ta and Ti in an oxygen ambient atmosphere (1×10^{-6} mbar) at a sample temperature of 800 K, following a recipe recently developed in our research group [23]. Subsequently, a TiO$_2$(110) film (100 Å thick) was grown on the blocking layer by deposition of Ti under the same conditions as those employed for the preparation of the blocking layer. Vanadium was added to the TiO$_2$(110) layer either by vanadium co-deposition during the growth of the TiO$_2$(110) layer or by deposition of vanadium onto the TiO$_2$(110) in O$_2$. The final step was to anneal the sample in ultrahigh vacuum (2×10^{-10} mbar) at 800 K for 10 min. Both ways of vanadium doping lead to essentially identical Ti + V mixed oxide layers since during annealing in vacuum vanadium dilutes into the layer due to its high diffusion speed at 800 K. The vanadium admixture concentrations C given in this publication are ratios of cross-section weighted intensities calculated from XPS spectra: $C = I_{V\,2p}/(I_{V\,2p} + I_{Ti\,2p})$.

3. Results and discussions

3.1 Surface structure of TiO$_2$(110) mixed with vanadium

The surface structure of the mixed oxide layers was studied with STM and LEED. Fig. 1 shows STM images of a TiO$_2$(110) thin film without, with 2% and with 8% of vanadium. Flat terraces with sizes of tens of nm are found on the (1 × 1) surface of the pure TiO$_2$ thin film after annealing in vacuum at 800 K for 10 min. When 2% of vanadium is introduced, rod-like structures along [0 0 1] (2 nm to 20 nm long) appear on the flat terraces. Apart from these structures, the surface has the typical (1 × 1) TiO$_2$(110) structure as shown in the inset in Fig. 1(b) in which a square and a circle mark two different bright spots on the dark O rods. Protrusions of the type marked by a square are usually assigned to bridging oxygen vacancies (BOVs) [28]. The density of such structures is about 15% per unit cell, higher than the 7% found for the TiO$_2$(110) thin film surface after annealing in vacuum at 800 K for 10 min [23].

The bright spot marked by a circle is attributed to a hydroxyl group resulting from the dissociation of water (from the residual gas atmosphere) at the surface. The rod-like structures centered above the bright Ti rods are about 1.2 nm wide and 0.3 nm high, which is identical to what has been reported for the "Ti_2O_3 rods" at (1 × 2) reconstructed surfaces of strongly reduced TiO_2(110) [29].
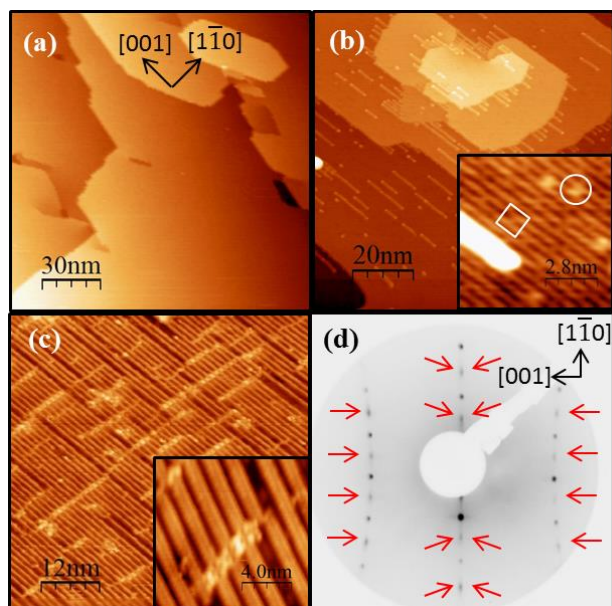
Fig. 1. (a) STM image of a TiO_2(110) thin film without vanadium. (b) STM image of a TiO_2(110) thin film with 2% of vanadium. The inset (8 nm × 8 nm) shows the atomically resolved (1 × 1) surface with an oxygen vacancy marked by a square and a hydroxyl group by a circle. (c) STM image of a TiO_2(110) thin film with 8% of vanadium. The inset (12 nm × 12 nm, somewhat distorted due to thermal drift) shows an excerpt of the image. (d) LEED pattern of the sample whose STM image is shown in panel (c). Red arrows mark the spots of the (1 × 2) superstructure. All layers were annealed in vacuo for 10 min at 800 K prior to recording the STM images.

When more vanadium (8%) is introduced into the TiO_2 thin film, more and longer rods along [0 0 1] show up together with cross-links along [$1\bar{1}0$] as shown in Fig. 1(c). The smallest distance between two neighboring rods is about 1.3 nm, which is twice the (1 × 1) lattice parameter (0.65 nm) along [$1\bar{1}0$]. This periodicity is reflected in the LEED pattern in Fig. 1(d) by (1 × 2) type superstructure spots. Distances larger than 1.3 nm between two neighboring rods are responsible for the diffuse intensity bridges between the regular TiO_2(110) spots along [$1\bar{1}0$]. The uniform appearance of the rods [see inset in Fig. 1(c)] is a vague indication that they contain just one type of metal ions, either vanadium or titanium.

The STM images shown here are very similar to STM images of heavily reduced (1 × 2) reconstructed TiO$_2$(110) surfaces [29–31], which is a good indication that the rods seen in the STM images in Fig. 1 just contain titanium.

The (1 × 2) reconstruction of regular TiO$_2$(110) (without vanadium) results from a strong reduction of the sample. It may be prepared by high temperature annealing in vacuo at temperatures in the range of 1300 K [29–31]. In our case of TiO$_2$(110) with dissolved vanadium, mild annealing at 800 K for 10 min was sufficient to prepare this reconstruction while it did not form on the surface of the vanadium free TiO$_2$(110) after the same annealing treatment (see Fig. 1). Apparently the (1 × 2) reconstruction of the Ti + V mixed oxide layer surface is a consequence of the vanadium admixture to the TiO$_2$(110) thin film.

3.2 Origin of the increased reducibility

Fig. 2 displays Ti 2p and V 2p core level XPS spectra of TiO$_2$(110) with admixed vanadium. Spectra of an oxidized surface (annealed in 2×10^{-6} mbar O$_2$ at 850 K for 1 min) are compared to spectra of a reduced surface (annealed in vacuo at 850 K for 5 min). At a photon energy of 630 eV the information depth of V 2p and Ti 2p spectra is 5-6 Å for 0° detection angle and only ~2 Å for a detection angle of 80° which means that in the latter case the spectra are strongly dominated by electrons from the topmost surface layer whereas electrons from deeper layers contribute more in the spectra recorded at 0°. Annealing in oxygen led to band bending which shifted all levels by 0.5 eV to lower binding energy. Therefore the energy scales in the graphs showing spectra of oxidized surfaces were shifted such that the Ti 2p binding energies were 459.0 eV like in the spectra of reduced surfaces.
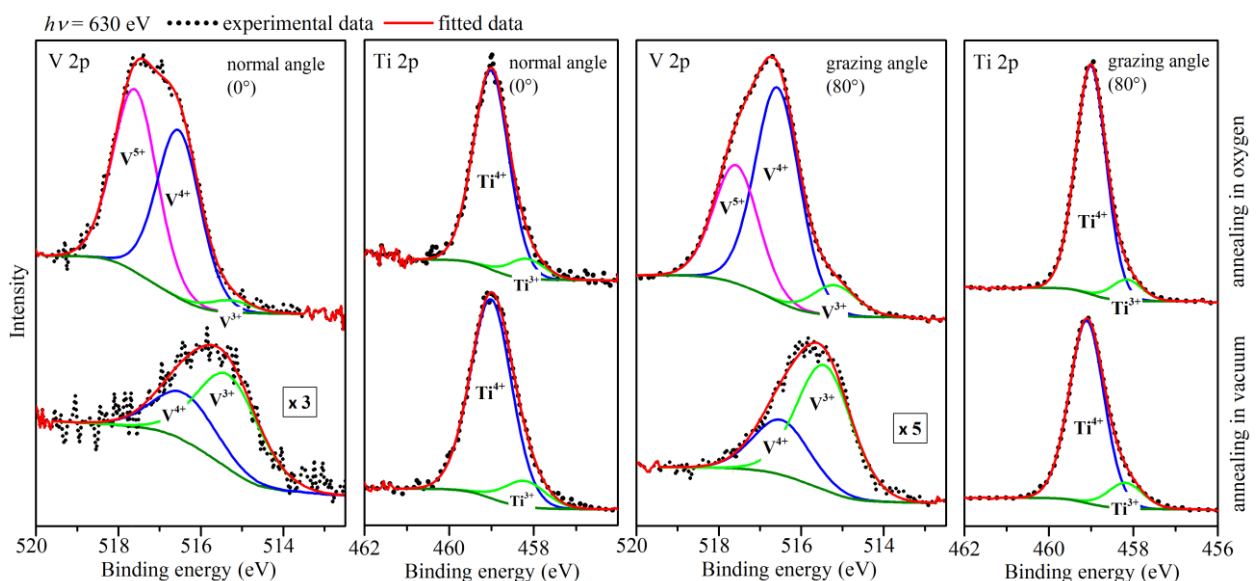
Fig. 2. V 2p and Ti 2p core level XPS spectra of a TiO_2(110) layer with admixed vanadium (concentrations are listed in Table 1). The spectra at the top were recorded after annealing the layer in 2×10^{-6} mbar of O_2 at 850 K for 1 min; the ones at the bottom were recorded after annealing in vacuum at 850 K for 5 min. The photon energy was 630 eV for all spectra. Electron detection angles of 0° and 80° with respect to the surface normal were employed. All spectra were fitted by two or three Gaussian-Lorentzian functions with a Shirley-type background subtracted before fitting. The count rates in the V 2p spectra of the reduced surfaces were multiplied by factors of 3 and 5, respectively, in order to compensate for the low emission intensities.

Table 1. Relative concentrations of vanadium and titanium ions with different oxidation states as obtained from the spectra shown in Fig. 2. The binding energies listed in this table result from peak fitting of the spectra.
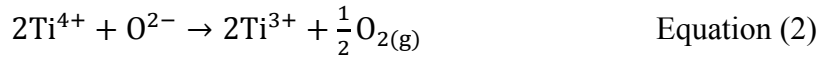
oxidation state		V^{5+}	V^{4+}	V^{3+}	V	Ti^{4+}	Ti^{3+}	Ti
binding energy (eV)		517.6	516.5	515.3		459.0	458.2	
annealing in O_2	%V (80°)	22	40	5	**67**	30	3	**33**
	%V (0°)	33	30	2	**65**	32	3	**35**
annealing in vacuum	%V (80°)	0	4	8	**12**	77	11	**88**
	%V (0°)	0	8	15	**23**	68	9	**77**

The Ti 2p and V 2p peaks were fitted by two or three mixed Gaussian-Lorentzian functions. Binding energies close to the literature values were obtained from the fits for Ti (Ti^{4+}, Ti^{3+}) and V (V^{5+}, V^{4+} and V^{3+}) [32–35]. Results are listed in Table 1. The numbers show that the concentration of vanadium at the oxidized surface (65%, 0°) is much higher than at the reduced surface (23%, 0°), and that in the case of the reduced surface, the concentration of vanadium at the surface is lower than below it as concluded from the concentrations obtained for different detection angles (23% for 0° vs 12% for 80°). This means that the vanadium tends to agglomerate at the surface in case of annealing in oxygen while reduction by annealing in vacuum leads to a situation where the vanadium ions avoid the surface. The overall vanadium concentration was less in the layers whose surface STM images are shown in Fig. 1, which is probably the reason why the images do not exhibit any clear indication of the presence of vanadium atoms at the surface at all.

Most of the vanadium atoms have a V^{4+} or V^{5+} oxidation state after annealing in oxygen while there is no V^{5+} in the reduced oxide. The concentration ratio $[V^{3+}]/[V^{4+}]$ for the reduced oxide is ~2 for both detection angles. The corresponding concentration ratio for the titanium ions ($[Ti^{3+}]/[Ti^{4+}]$) is 0.13-0.14 which shows that reduction affects the vanadium ions much more than the titanium ions. Table 1 shows that the Ti^{3+} and V^{3+} concentrations in the reduced layer are not too different (some percent difference should be not be taken too serious since the error margin for the Ti^{3+} concentrations is surely significant since the Ti^{3+} peaks are just weak shoulders in the Ti 2p structures in Fig. 2) which indicates that the reduction may occur via the following reaction:

$$Ti^{4+} + V^{4+} + O^{2-} \rightarrow Ti^{3+} + V^{3+} + \frac{1}{2}O_{2(g)} \qquad \text{Equation (1)}$$
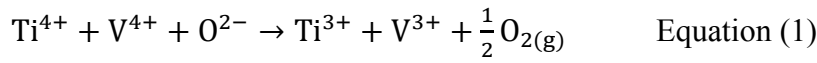
as opposed to the mechanism for a layer without vanadium:

$$2Ti^{4+} + O^{2-} \rightarrow 2Ti^{3+} + \frac{1}{2}O_{2(g)} \qquad \text{Equation (2)}$$

The reduction according to equation (1) would produce Ti^{3+} and V^{3+} in equal amounts, in rough agreement with the numbers listed in Table 1. We note that the Ti 2p spectra of the reduced mixed oxide layer in Fig. 2 are similar to spectra measured for a regular $TiO_2(110)$ (1 × 2) surface [12,32,36], consistent with similar degrees of reduction.

The fourth atomic ionization energies are 46.71 eV for vanadium ($V^{3+} \rightarrow V^{4+}$) and 43.08 eV for titanium ($Ti^{3+} \rightarrow Ti^{4+}$) [37,38], which is a hint that the reduction of vanadium in TiO_2 might cost less energy than the reduction of Ti which would lead to an enhanced reducibility of TiO_2 with admixed vanadium, as experimentally observed. This simple picture may be somewhat reasonable since vanadium ions occupy the same lattice sites as titanium ions according to a recent photoelectron diffraction study [24]. We note that VO_2 (rutile structure) has a bulk oxygen vacancy formation energy of 3.53 eV [39], somewhat lower than the corresponding value ($\geq$ 4.35 eV) for TiO_2 [40], which is a further indication that a reduction process involving vanadium ions is energetically preferred.

The formation energies of BOVs at the (110) surfaces of regular and V-doped TiO_2 have recently been calculated by Kim et. al. with DFT slab calculations [41]. In their model a vanadium atom replaces a 5-fold coordinated surface Ti atom. According to their results, the energy to remove a certain bridging oxygen atom from the neighborhood of a 5-fold coordinated V atom is 3.37 eV which is lower than the energy of 3.72 eV for pure $TiO_2(110)$. While this model is not strictly applicable to the current situation, since the vanadium atoms

prefer to stay below the very surface in the case of a reduced mixed oxide, it is nevertheless another indication that the introduction of vanadium into TiO_2 may result in an increased reducibility. The observation that vanadium prefers a location below the surface is in accord with the results of a calculation by Asaduzzaman and Krueger who found that vanadium atom prefer substitutional sub-surface sites over surface sites [42].

Nitrogen and chromium doping also affect the defect density in $TiO_2(110)$ [20,43]. A (1×2) reconstruction was observed in the case of nitrogen doping by implantation. It was assumed that the higher charge of nitrogen (N^{3-}) relative to that of oxygen (O^{2-}) results in oxygen vacancies to maintain charge neutrality [19]. Lattice stress minimization and again charge neutrality were assumed to be responsible for an enhanced concentration of oxygen vacancies in the case of doping with chromium [20]. In the here-discussed case of a vanadium admixture, the lattice stress will be rather small since the ionic radii of V^{3+} and V^{4+} are close to those of their titanium counterparts [44], and V^{5+} does probably not exist in significant concentrations below the surface [24]. Therefore we assume (as discussed before) that a lower energy for the reduction of V^{4+} relative to that of Ti^{4+} is responsible for the increased reducibility in the present case.

3.3 Reactivity test with methanol adsorption

The chemical activity of the mixed oxide layers was examined with TPD using methanol as the probe molecule. Fig. 3(a) displays TPD spectra recorded for methanol adsorbed on a layer with 2% of vanadium. Methanol (*m/z*=31) has major desorption peaks at 350 K and 680 K. Water (*m/z*=18) desorbs at 500 K, and formaldehyde (m/z=30) desorption is found at 680 K. There is also a weak methane signal (*m/z*=15) at about 700 K while ethylene (*m/z*=27) intensity higher than the noise level of the spectrometer is not observed. These results are similar to results reported for a $TiO_2(110)$ layer without vanadium except that the intensities are somewhat different [23].
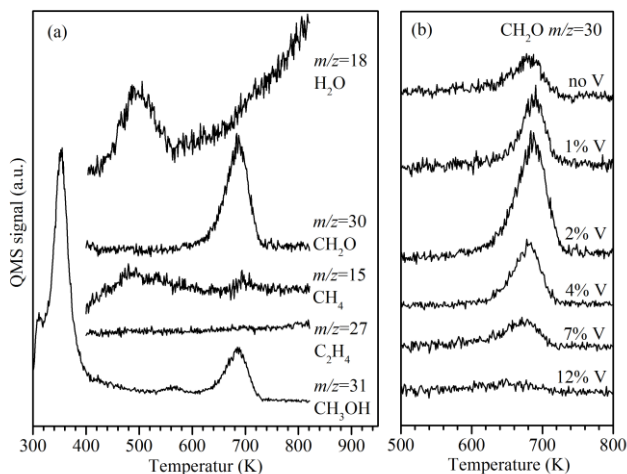
Fig. 3. (a) TPD spectra of 50 L of methanol adsorbed at room temperature onto a $TiO_2(110)$ layer with 2% of vanadium. (b) TPD spectra (mass 30) of methanol on a $TiO_2(110)$ thin film with different vanadium concentrations (0%, 1%, 2%, 4%, 7% and 12%).

Formaldehyde TPD spectra of (m/z=30) for different vanadium concentrations are shown in Fig. 3(b). The intensity of the peak at 680 K is highest for 2% of vanadium and decreases when the vanadium concentration is increased beyond this level or decreased below it. The amount of formaldehyde produced by a film with 7% of vanadium is approximately the same as the amount produced by the pure TiO_2 thin film while the amount is near to zero when the layer contains 12% of vanadium.

According to TPD studies of methanol on $TiO_2(110)$, the desorption of formaldehyde at 680 K is related to methoxy groups bound to BOV sites [23,45,46]. The large amount of formaldehyde desorbing from the film with 2% of vanadium reflects the high concentration of BOV sites at the surface of this film, which is about 15% as estimated from the STM image in Fig. 1(b). The BOV density at the surface of the layer without vanadium is only 7% which leads to the smaller intensity of the formaldehyde desorption peak in Fig. 3(b). The surface of the layer with 12% of vanadium is largely covered with the (1×2) reconstruction. There are not many BOVs but many "Ti_2O_3" rods which are apparently chemically inactive. The TPD data do only exhibit structures which are also known for methanol on regular $TiO_2(110)$ without vanadium which is a strong indication that there is no direct methanol-vanadium interaction, supporting the conclusion obtained from the XPS measurements that vanadium atoms are mostly located below the surface.

STM images recorded after adsorption of 50 L of methanol at 300 K provide further insight into the chemical activity of the mixed oxide layer. Methoxy groups bound to BOVs and hydroxyl groups were the only methanol-related species at the surface since it was flashed to 400 K before the images were recorded. The images exhibit only a few methanol-induced protrusions on the (1×2) rods [see Fig. 4(b)], indicating that the rods are essentially inactive for formaldehyde production, in agreement with the conclusions drawn from the TPD experiments. Fig. 4(c) shows that the area between the rods is densely covered with methanol related species. The height profile in shown Fig. 4(d) reveals species with two different heights (0.6 Å and 1.5 Å) which, following a comparison with literature values [28,47–49], are attributed to hydroxyl and methoxy groups, respectively. The density of the hydroxyl/methoxy groups is about 15% relative to the density of surface unit cells which is the same as the density of BOVs found for the film doped with 2% of vanadium, which gave the highest yield of formaldehyde in the TPD experiments.
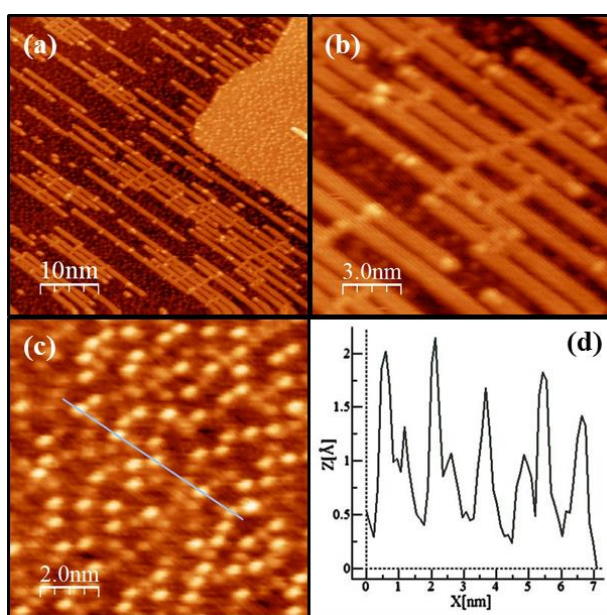
Fig. 4. (Color online) (a) STM image of a $TiO_2(110)$ film with 2% of vanadium exposed to 50 L of methanol at 300 K. Prior to scanning the sample was flashed to 400 K to desorb molecularly adsorbed methanol. (b) Part of image (a) containing mainly (1×2) rods. (c) Part of image (a) showing an area without (1×2) rods. (d) Height profile measured along the line in image (c).

4. Conclusions

We have successfully prepared Ti + V mixed oxide layers with the vanadium ions locked in the layers by a diffusion blocking barrier between the $TiO_2(110)$ single crystal substrate and the overlayer. We found that the vanadium atoms prefer sub-surface sites in reduced layers, while vanadium concentrates at the surface when the layers are annealed in oxygen. The presence of vanadium ions increases the reducibility of the layers which leads to a high density of reduction related features at the surface even after a rather mild annealing at 800 K for some minutes. When a small amount of vanadium (e.g. 2%) is introduced into a layer, a high density of BOVs is produced by annealing at 800 K for some minutes. These BOVs are responsible for a large amount of formaldehyde produced by annealing a methanol covered surface to 680 K. When more vanadium ($\geq$ 8%) is dissolved in the layer, annealing at 800 K produces a (1 × 2) reconstruction with cross-links as known for heavily reduced $TiO_2(110)$. The (1 × 2) related rod-like surface structures appear to be largely inactive with respect to formaldehyde production. We assume that a smaller energy for the removal of oxygen from the vicinity of vanadium atoms in the $TiO_2(110)$ layer is responsible for the increased reducibility.

References

[1]   L. Lefferts, K. Seshan, B. Mojet, J. Van Ommen, Non-conventional oxidation catalysis, Catal. Today. 100 (2005) 63–69.

[2]   G. Pacchioni, Modeling doped and defective oxides in catalysis with density functional theory methods: Room for improvements, J. Chem. Phys. 128 (2008) 182505.

[3]   E.W. McFarland, H. Metiu, Catalysis by doped oxides, Chem. Rev. 113 (2013) 4391–4427.

[4]   N. Nilius, H.-J. Freund, Activating nonreducible oxides via doping, Acc. Chem. Res. 48 (2015) 1532–1539.

[5]   a Cimino, R. Bosco, V. Indovina, M. Schiavello, Decomposition of nitrous oxide upon nickel oxide-magnesium oxide solid solutions, J. Catal. 5 (1966) 271–278.

[6]   X. Shao, S. Prada, L. Giordano, G. Pacchioni, N. Nilius, H.J. Freund, Tailoring the shape of metal Ad-particles by doping the oxide support, Angew. Chemie - Int. Ed. 50 (2011) 11525–11527.

[7]   I. Yeriskin, M. Nolan, Doping of ceria surfaces with lanthanum: a DFT + U study, J. Phys. Condens. Matter. 22 (2010) 135004.

[8]   Y. Cui, X. Shao, M. Baldofski, J. Sauer, N. Nilius, H.-J. Freund, Adsorption, activation, and dissociation of oxygen on doped oxides, Angew. Chemie - Int. Ed. 52 (2013) 11385–11387.

[9]   F. Stavale, X. Shao, N. Nilius, H.-J. Freund, S. Prada, L. Giordano, G. Pacchioni, Donor characteristics of transition-metal-doped oxides: Cr-doped MgO versus Mo-doped CaO, J. Am. Chem. Soc. 134 (2012) 11380–11383.

[10]   H.-J. Freund, G. Pacchioni, Oxide ultra-thin films on metals: new materials for the design of supported metal catalysts., Chem. Soc. Rev. 37 (2008) 2224–2242.

[11]   N. Isomura, X. Wu, Y. Watanabe, Atomic-resolution imaging of size-selected platinum clusters on TiO_2(110) surfaces, J. Chem. Phys. 131 (2009) 4–7.

[12]   J. Abad, C. Rogero, J. Mendez, M. Lopez, J. Martin-Gago, E. Roman, Ultra-thin Si overlayers on the TiO_2(110)-(1×2) surface: Growth mode and electronic properties, Surf. Sci. 600 (2006) 2696–2704.

[13]   O. Karslıoğlu, X. Song, H. Kuhlenbeck, H. Freund, Mo+TiO_2(110) Mixed Oxide Layer: Structure and Reactivity, Top. Catal. 56 (2013) 1389–1403.

[14]   D. Matthey, J.G. Wang, S. Wendt, J. Matthiesen, R. Schaub, E. Lægsgaard, B. Hammer, F. Besenbacher, Enhanced Bonding of Gold Nanoparticles on Oxidized TiO2(110), Science (80-.). 315 (2007) 1692–1696.

[15]   A. Fujishima, X. Zhang, D.A. Tryk, TiO_2 photocatalysis and related surface phenomena, Surf. Sci. Rep. 63 (2008) 515–582.

[16]   U. Diebold, The surface science of titanium dioxide, Surf. Sci. Rep. 48 (2003) 53–229.

[17]   M.A. Henderson, A surface science perspective on TiO_2 photocatalysis, Surf. Sci. Rep. 66 (2011) 185–297.

[18]   M. Zamora, T. López, R. Gómez, M. Asomoza, R. Melendrez, Oligomerization of acetone over titania-doped catalysts (Li, Na, K and Cs): Effect of the alkaline metal in activity and selectivity, in: Catal. Today, 2005: pp. 289–293.

[19]   M. Batzill, E.H. Morales, U. Diebold, Influence of Nitrogen Doping on the Defect

Formation and Surface Properties of TiO_2 Rutile and Anatase, Phys. Rev. Lett. 96 (2006) 026103.

[20] R. Bechstein, M. Kitta, J. Schütte, A. Kühnle, H. Onishi, Evidence for Vacancy Creation by Chromium Doping of Rutile Titanium Dioxide (110), J. Phys. Chem. C. 113 (2009) 3277–3280.

[21] J. Biener, M. Bäumer, J. Wang, R.J. Madix, Electronic structure and growth of vanadium on TiO_2(110), Surf. Sci. 450 (2000) 12–26.

[22] S. Agnoli, C. Castellarin-Cudia, M. Sambi, S. Surnev, M.G. Ramsey, G. Granozzi, F.P. Netzer, Vanadium on TiO_2(110): adsorption site and sub-surface migration, Surf. Sci. 546 (2003) 117–126.

[23] X. Song, E. Primorac, H. Kuhlenbeck, H.-J. Freund, Decoupling a thin well-ordered TiO_2(110) layer from a TiO_2(110) substrate with a Ti + Ta mixed oxide interlayer, J. Phys. Chem. C. 120 (2016) 8185–8190.

[24] D. a. Duncan, D. Kreikemeyer-Lorenzo, E. Primorac, O. Karslioğlu, M. Naschitzki, W. Unterberger, H. Kuhlenbeck, D.P. Woodruff, V-doped TiO2(110): Quantitative structure determination using energy scanned photoelectron diffraction, Surf. Sci. 630 (2014) 64–70.

[25] J.F. Moulder, W.F. Stickle, P.E. Sobol, K.D. Bomben, Handbook of X-ray Photoelectron Spectroscopy, Perkin-Elmer Corporation, Eden Prairie, USA, 1992.

[26] I. Horcas, R. Fernández, J.M. Gómez-Rodríguez, J. Colchero, J. Gómez-Herrero, a. M. Baro, WSXM: A software for scanning probe microscopy and a tool for nanotechnology, Rev. Sci. Instrum. 78 (2007).

[27] P. Feulner, D. Menzel, Simple ways to Improve "Flash desorption" Measurements from single crystal surfaces, J. Vac. Sci. Technol. 17 (1980) 662–663.

[28] S. Wendt, R. Schaub, J. Matthiesen, E.K. Vestergaard, E. Wahlström, M.D. Rasmussen, P. Thostrup, L.M. Molina, E. Lægsgaard, I. Stensgaard, B. Hammer, F. Besenbacher, Oxygen vacancies on TiO_2(110) and their interaction with H_2O and O_2: A combined high-resolution STM and DFT study, Surf. Sci. 598 (2005) 226–245.

[29] H. Onishi, Y. Iwasawa, Reconstruction of TiO_2(110) surface: STM study with atomic-scale resolution, Surf. Sci. 313 (1994) L783–L789.

[30] M. Bowker, R. a Bennett, The role of Ti^{3+} interstitials in TiO_2(110) reduction and oxidation, J. Phys. Condens. Matter. 21 (2009) 474224–474232.

[31] C.M. Yim, C.L. Pang, G. Thornton, Probing the local electronic structure of the cross-linked (1×2) reconstruction of rutile TiO_2(110), Surf. Sci. (2015)

http://dx.doi.org/10.1016/j.susc.2015.04.022.

[32] W. Göpel, J.A. Anderson, D. Frankel, M. Jaehnig, K. Phillips, J.A. Schäfer, G. Rocker, Surface defects of TiO_2(110): a combined XPS, XAES and ELS study, Surf. Sci. Lett. 139 (1984) A129.

[33] U. Diebold, T.E. Madey, U. Diebold, TiO_2 by XPS, Surf. Sci. Spectra. 4 (1996) 227–231.

[34] G. Silversmit, D. Depla, H. Poelman, G.B. Marin, R. De Gryse, Determination of the V2p XPS binding energies for different vanadium oxidation states (V^{5+} to V^{0+}), J. Electron Spectros. Relat. Phenomena. 135 (2004) 167–175.

[35] N.J. Price, J.B. Reitz, R.J. Madix, E.. Solomon, A synchrotron XPS study of the vanadia–titania system as a model for monolayer oxide catalysts, J. Electron Spectros. Relat. Phenomena. 98-99 (1999) 257–266.

[36] L.-Q. Wang, D.R. Baer, M.H. Engelhard, Creation of variable concentrations of defects on TiO_2(110) using low-density electron beams, Surf. Sci. 320 (1994) 295–306.

[37] A.M. James, M.P. Lord, Macmillan's Chemical and Physical Data, Macmillan Press, Basingstoke, UK, 1992.

[38] J.E. Huheey, E.A. Keiter, R.K. Harper, Inorganic Chemistry: Principles of Structure and Reactivity, 4th ed, Harper Collins, New York, USA, 1993.

[39] T.A. Mellan, R. Grau-crespo, Density functional theory study of rutile VO_2 surfaces, J. Chem. Phys. 137 (2012) 154706.

[40] T. Pabisiak, A. Kiejna, Energetics of oxygen vacancies at rutile TiO_2(110) surface, Solid State Commun. 144 (2007) 324–328.

[41] H.Y. Kim, H.M. Lee, R.G.S. Pala, V. Shapovalov, H. Metiu, CO Oxidation by Rutile TiO_2(110) Doped with V, W, Cr, Mo, and Mn, J. Phys. Chem. C. 112 (2008) 12398–12408.

[42] A. Asaduzzaman, P. Krueger, Adsorption and Cluster Growth of Vanadium on TiO2(110) Studied by Density Functional Theory, J. Phys. Chem. C. 2 (2008) 4622–4625.

[43] M. Batzill, E.H. Morales, U. Diebold, Influence of Nitrogen Doping on the Defect Formation and Surface Properties of TiO_2 Rutile and Anatase, Phys. Rev. Lett. 96 (2006) 026103–026106.

[44] R.D. Shannon, Revised effective ionic radii and systematic studies of interatomic distances in halides and chalcogenides, Acta Crystallogr. A32 (1976) 751–767.

[45] Q. Wang, R.J. Madix, Partial oxidation of methanol to formaldehyde on a model

supported monolayer vanadia catalyst: Vanadia on $TiO_2(110)$, Surf. Sci. 496 (2002) 51–63.

[46] G.S. Wong, M.R. Concepcion, J.M. Vohs, Reactivity of monolayer V_2O_5 films on $TiO_2(110)$ produced via the oxidation of vapor-deposited vanadium, Surf. Sci. 526 (2003) 211–218.

[47] X.F. Cui, Z. Wang, S.J. Tan, B. Wang, J.L. Yang, J.G. Hou, Identifying Hydroxyls on the $TiO_2(110)$-1×1 Surface with Scanning Tunneling Microscopy, J. Phys. Chem. C. 113 (2009) 13204–13208.

[48] Z. Zhang, O. Bondarchuk, J.M. White, B.D. Kay, Z. Dohnálek, Imaging adsorbate O-H bond cleavage: methanol on $TiO_2(110)$, J. Am. Chem. Soc. 128 (2006) 4198–9.

[49] C. Zhou, Z. Ren, S. Tan, Z. Ma, X. Mao, D. Dai, H. Fan, X. Yang, J. Larue, R. Cooper, A.M. Wodtke, Z. Wang, Z. Li, B. Wang, J. Yang, J. Hou, Site-specific photocatalytic splitting of methanol on $TiO_2(110)$, Chem. Sci. 1 (2010) 575–580.